RSC Advances

ROYAL SOCIETY OF CHEMISTRY

www.rsc.org/advances

A comparative computational study on the synthesis prescriptions, structures and acid properties of B, Al and Ga incorporated MTW-type zeolites

Authors:

Gang Feng [a], Deqin Yang [a], Dejin Kong [a,*], Jianwen Liu[b,*], Zhang-Hui Lu[c,*]

Affiliation:

[a] *Shanghai Research Institute of Petrochemical Technology SINOPEC, 201208, Shanghai, P.R.China*

[b] *National Supercomputing Center in Shenzhen, 518055, Shenzhen, P.R. China*

[c] *College of Chemistry and Chemical Engineering, Jiangxi Normal University, Nanchang, 330022, P.R. China*

Corresponding authors:

Jianwen Liu Tel:+86 755 86576112; fax: +86 755 86576000; Email: liujw@nsccsz.gov.cn

Dejin Kong Tel:+86 21 68462542; fax:+86 21 68462283; Email: kongdj.sshy@sinopec.com

Zhang-Hui Lu Tel: +86 791 88121974; fax: +86 791 88120843; Email: luzhanghui@hotmail.com

Highlights:

1, The trivalent and alkaline metal ions are favored following the order: Al > Ga > B, Li > K ≈ Na > NH_4 > H for the synthesis of MTW zeolites.

2, Different M–O bond properties were observed for B, Al and Ga incorporated MTW zeolites: covalent B–O bonds, ionic Al–O bonds, in between Ga–O bonds.

3, Alkaline metal ions significantly change the cell volumes of B, Al and Ga incorporated MTW zeolites: H-form are larger than Li-form, while smaller than K-form.

4, The Brønsted acidity follow the order: HB-MTW < HGa-MTW < HAl-MTW.

Abstract: The B, Al and Ga incorporated H-, NH_4-, Li-, Na- and K-forms MTW zeolites were comparatively studied to understand the crystallization thermochemistry, structure stabilities and acid properties using dispersion corrected density functional theory. Substitution energies were introduced to evaluate the synthesis prescriptions for MTW zeolites. The calculated results show that the trivalent and alkaline metal ions for the synthesis of the MTW zeolites are favored following the order: Al > Ga > B and Li > K ≈ Na > NH_4 > H. The B–O, Si–O and O–H bonds show covalent property whereas the Al–O bonds show obvious ionic property. However, the Ga–O bonds show the property between the Al–O and B–O bonds. The introducing of alkaline metal ions significantly changes the cell volumes. As a result, the cell volumes of the H-form B, Al and Ga incorporated MTW zeolites are larger than Li-form while smaller than K-form MTW zeolites. Further property studies show that the Brønsted acid sites of the zeolites follow the order of HAl-MTW > HGa-MTW > HB-MTW. The Lewis acidity of HB-MTW is similar to that of HAl-MTW, while weaker than HGa-MTW. These results are in well agreement with the previous experiments and provide new insight for the MTW zeolites.

Key words: Substitution energy, MTW-type zeolite, Adsorption, Density functional theory

1. Introduction

Zeolites are crystalline microporous materials with tetrahedrally-coordinated framework structures incorporating well-defined channel systems and cavities.[1-3] The MTW-type zeolites, which is in the monoclinic space *C2/m* with a = 25.552 Å, b = 5.256 Å, c = 12.117 Å and β = 109.312º, was first synthesized by Rosinski and Rubin.[4] It was reported that each unit cell of the MTW-type zeolites contains $Si_{28}O_{56}$. The pores of MTW-type zeolites are one-dimensional 12-membered ring channels along the b axis without intersections.[5,6] Because of their outstanding solid-acid,[7-12] adsorption-desorption properties for small molecules,[13] and shape-selectivity properties,[14] the MTW-type zeolites are considered great potential in many hydrocarbon conversion reactions, i.e. benzene alkylation reaction,[15] methylation of naphthathene with methanol,[16,17] and the conversion of methanol-to-olefins.[18]

Due to its wide applications in catalysis, many previous works have investigated the synthesis, acid properties and the applications of the MTW-type zeolites.[10,15-31] Attentions were paid to the new synthesis methods for the incorporation of various heteroatoms (Al, Ga, Fe and B) into the zeolites framework, since the incorporated trivalent cations could change the acid properties of the zeolite with little side-effects on the pore structure.[10,16,22,23,30,31]

For the most intensively investigated Al-MTW zeolite, the lowest Si/Al ratio of about 30 could be achieved with organic structure directing agents (OSDA) as templates.[10,22] The infrared bands at 3610 and 3575 cm^{-1} were tentatively attributed to hydroxyl groups vibrating in the main channel and in the six-membered rings of the Si–OH–Al structure of Al-MTW, respectively.[10] Okubo et al. reported the seeds assisted OSDA-free method for the preparation of the Al-MTW zeolite and acquired the lowest Si/Al of about 10.[27,28] They also found that Li advantageously contributed to the synthesis of Al-MTW zeolite than Na cation.[29] Smirniotis et al. investigated the acid properties of ZSM-12 using infrared spectroscopy, and NH_3-stepwise temperature-programmed desorption (STPD).[12] They found that the synthesized ZSM-12

sample possesses a small number of Lewis acid sites, and ammonia desorbs completely from those Lewis sites upon an increase of temperature above 150 ºC. Araujo et al. investigated the acid properties of HZSM-12 via n-butylamine thermodesorption.[20] They concluded that the HZSM-12 zeolite presents two kinds of acid sites, with apparent activation energy for n-butylamine desorption in the ranges of 115~125 and 230~250 kJ•mol^{-1}, classified as weak and strong acid, respectively. The temperature ranges of 100~330 °C and 330~550°C relate to n-butylamine desorption from the weak and strong acid sites, respectively. The total acidity indicated that there is approximately one n-butylamine molecule adsorbed to each aluminum atom in the zeolite. However the apparent activation energy for n-butylamine desorption for the same kinds of acid sites were practically identical for samples with different Si/Al molar ratio, indicating that the Al concentration influences only the amount of acid sites.

The synthesis of Fe-MTW zeolites were also reported by Košová and Čejka using triethylmethylammonium bromide as OSDA.[10] They found that the minimum Si/Fe ratio achieved for Fe-MTW is around 37, which is very close to the minimum Si/Al ratio of 35 for Al-MTW. In addition, they also found that both the Brønsted and Lewis acid sites are present in significant concentrations in all Al-MTW and Fe-MTW zeolites. The highest concentrations of Brønsted sites were observed for the zeolites of low Si/Al and Si/Fe ratios. The infrared bands at 3630 and 3590 cm^{-1} were observed for the Fe-MTW zeolites, which indicates the difference of acid strengths of the HFe-MTW from HAl-MTW.

The synthesis of Ga-MTW zeolites was reported within the Si/Ga ratio in the range of 60~120.[31] It was also found that the thermal stability of tetrahedral Ga is good since no extra framework octahedral Ga was detected after activation at 823 K, and the NH_3-TPD experiment showed that the acid properties of the H-form Ga-MTW is slightly less than those of the Al analog, which are comparable to those developed by HZSM-5.

Compared to the Al, Fe and Ga incorporated zeolites, B incorporated zeolites display a

lower acidic strength, a property which can be appropriately exploited for modulating the catalytic properties of acidic catalysts.[32] The synthesis of B-MTW zeolites in hydrothermal condition was reported using Na as the alkaline metal ion, and the NMR characterization shows that the B atoms were incorporated into the zeolite framework as tetrahedron of $B(OSi)_4$.[30] It was reported that the B incorporated zeolites show weaker acid properties than the Al, Fe and Ga incorporated zeolites for the MFI and MOR,[33-35] while the acid properties of B-MTW zeolites were not investigated.

Though the previous experiments synthesized the Al, B and Ga incorporated MTW-type zeolites, and demonstrated that the acid properties of the zeolites could be efficiently adjusted via incorporation of different trivalent ions. The influences of the different trivalent and alkaline metal ions to the thermo-chemistry of the zeolites synthesis processes,[36] structures and the acid properties of the zeolites were not well known at molecular level. In our previous works,[37-39] the thermochemistry for the MTW zeolites synthesis were tentatively investigated using dispersion corrected density functional theory (DFT). The results show that the thermochemistry for the MTW zeolites synthesis could be effectively described by the substitution energy for the substitution of one Si atom of the zeolites framework with one trivalent ion and an alkaline metal atom. The calculated Al location and acid properties of the zeolites agree well with the experimental results that Al could distributes in different sites of the framework.

Since the B, Al and Ga, which were usually used as the trivalent ions for zeolites synthesis, are in the same group of the elementary table and have the similar electronic structures. On the basis of our previous works,[37,38] the present work comparatively investigated the synthesis, structures and acid properties of B, Al and Ga incorporated MTW-type zeolites using dispersion corrected periodic DFT. Since different alkaline metal ions may seriously influence the crystallization of the zeolites,[40] the influences of the alkaline metal ions (K, Na, Li, H,

NH_4) to the thermochemistry of the zeolites synthesis reactions were investigated for the B, Al and Ga incorporated MTW zeolites. The acid properties of the B-MTW zeolite were investigated via NH_3 and pyridine adsorption. The results were analyzed and compared with our previous work on the Al-MTW zeolite.[38]

2. Computation details

DFT as implemented in the Vienna Ab initio Simulation Package (VASP) was applied.[41,42] The dispersive interactions were calculated using DFT-D2 method of Grimme.[43] Spin-polarized calculations were carried out with the PBE generalized-gradient exchange and correlation functional.[44] Core electrons were described by the projected augmented wave method (PAW).[45,46] The $p(1\times2\times1)$ cell was sampled with a 2×2×2 *k*-points mesh, generated by the Monkhorst-Pack algorithm. For structure optimizations, both the cell parameters and the atoms of MTW zeolites were fully relaxed. The convergence criteria were 1.0×10^{-4} eV, 1×10^{-3} eV and 0.05 eV/Å, respectively, for the SCF energy, total energy and atomic forces. The DFT-D2 parameters were set the same as Grimme proposed.[43,47,48] The gas phase molecules were calculated in 20×20×20 Å lattice.

The vibrational frequencies and normal modes were calculated by diagonalization of the mass-weighted force constant matrix, which was obtained using the method of finite differences of forces as implemented in VASP. The ions are displaced in the +/– directions of each Cartesian coordinate by 0.02 Å. All reported minimum energy structures have only real frequencies.

As we optimized the cell parameters together with the ions positions, the selection of the cutoff energy is essential for the reliability. To evaluate the reliability of cutoff energies, we took H-form Al-MTW as an example to calculate the changes of NH_3 adsorption energies and substitution energies with different cutoff energies as shown in Table 1. The results show that the changes of NH_3 adsorption energies (< 0.11 eV, 7.1%) and the substitution energies (<

0.06 eV, 3.5%) are small as the cutoff energy varying from 350 to 1000 eV, which shows that the cutoff energy of 350 eV can produce reliable results for the MTW system. In the following, a cutoff energy of 350 eV is used for all the calculations.

As shown in Figure 1, each unit cell ($Si_{28}O_{56}$) of the MTW-type framework contains 7 inequivalent Si and 11 inequivalent O sites. The inequivalent Si sites are indexed with numbers (1–7), and the inequivalent O sites are indexed with letters (a–k). To minimize the interaction of adsorbates (NH_3 and pyridine) of the neighboring cells, a $p(1\times2\times1)$ cell ($Si_{56}O_{112}$) was used for all calculations. In order to investigate the local structures of trivalent M (M = B, Al, Ga) ions in the zeolite, one Si atom was substituted by M atom in the $p(1\times2\times1)$ cell to get the Si/M ratio of 55. For the H-, Li-, Na-, K-, NH_4-forms MTW-type zeolites, structures with all possible M locations were systemically calculated. For the optimization of the zeolite, 7 inequivalent T sites of the zeolite were investigated for the substitution of Si by M. For M in each T sites, we tried to bond the H-, Li-, Na-, K- and NH_4 ions to the four different O sites near the M atom, and calculated the alkaline atoms pointing to different nearby O atoms in the input structures. The optimized local minima structures were used to investigate the adsorption of NH_3 and pyridine. Both the Lewis and Brønsted acid sites were calculated for the adsorption of NH_3 and pyridine. Furthermore, we also investigated the adsorption of NH_3 and pyridine in both the main channel and the small cages (See Figure 1) of the zeolite.

(Figure 1)

In order to study the influences of the trivalent M and alkaline metal ions Y (Y = K, Na, Li, H, NH_4) to the thermochemistry of the zeolites synthesis reactions, we calculated the reaction of 56 $Si(OH)_4$ molecules to produce a $p(1\times2\times1)$ MTW-type zeolites cell ($Si_{56}O_{112}$) and 112 H_2O molecules. It shows that the pure silica MTW zeolites synthesis reaction releases –18.25 eV energies, which indicates an exothermic reaction. The incorporation of one M (M = B, Al,

Ga) atom into the MTW framework could be considered as the substitution of one Si atom of the pure silica zeolites by one M and Y atoms, which described as the following reaction:

$$(\text{O-Si-O})_n^{\text{MTW}} + n\text{M(OH)}_3 + n\text{YOH} \rightarrow n\text{Si(OH)}_4 + (\text{O-M-OY})_n^{\text{MTW}} \quad \text{(a)}$$

where M = B, Al, Ga; Y = H, NH_4, Li, Na, K; n = 1, 2, 3, … The corresponding substitution energy could be calculated as following:

$$E_{sub} = nE[\text{Si(OH)}_4)] + E[(\text{O-M-OY})_n^{\text{MTW}}] - E[(\text{O-Si-O})_n^{\text{MTW}}] - nE[\text{M(OH)}_3] - nE[\text{YOH}] \quad \text{(b)}$$

Where $E[\text{Si(OH)}_4)]$, $E[(\text{O-M-OY})_n^{\text{MTW}}]$, $E[(\text{O-Si-O})_n^{\text{MTW}}]$, $E[\text{M(OH)}_3]$ and $E[\text{YOH}]$ are the total energies of the free $Si(OH)_4$, YM-MTW zeolite cell, pure silica MTW-type zeolite cell, free $M(OH)_3$ and YOH molecules, respectively. From the thermodynamical point of view, E_{sub} could be used to evaluate and pre-select the experimental prescriptions for zeolite synthesis and structure determination. For M-MTW as an example, for a given n, E_{sub} is a function of Y, a larger E_{sub} indicates a thermodynamically more preferred Y and M for the zeolite synthesis. For a given Y and M, E_{sub} is a function of n, a larger E_{sub} indicates preferred Si/M ratio for the zeolite. In addition, for n = 1, a larger E_{sub} indicates a more favored substitution T site for M and Y. It should be noted that the zeolite synthesis reactions in condense phase are rather complicated. The present substitution model is a simplified gas phase reaction, which has some correspondence to experimental conditions but it is quite different.

The adsorption energies (E_{ads}) for the adsorption of NH_3 and pyridine in the zeolite were calculated by

$$E_{ads} = E(\text{molecule@MTW}) - [E(\text{molecule}) + E(\text{MTW})] \quad \text{(c)}$$

where E(molecule@MTW), E(molecule) and E(MTW) are the total energies of the MTW-type zeolite cell with adsorbed molecule in the pore, the gas phase NH_3 or pyridine molecules and the MTW-type zeolite, respectively. The larger adsorption energy indicates the stronger adsorption on the acid site for the probe molecules.

3. Results and discussion

In order to evaluate the importance of the dispersion interaction to the results, the relative total energies and van der Waals energies for the structures of the H-form B, Al and Ga incorporated MTW zeolites were shown in Table 2 (The original total energies and van der Waals energies for all the discussed structures of the present work are shown in **Table S1-S3** in **Supplementary Materials**). Similar to our previous results on Al-MTW,[38] the van der Waals contribution to B-MTW and Ga-MTW are also very important, which significantly change the order of the relative stability. As shown in Table 2, both DFT and DFT-D2 indicate that the energy differences for B, Al and Ga in different T sites of the H-form MTW-type zeolite were small. However, the most stable substitution sites may be different. For example, the DFT-D2 indicates that T(4) are the most favored substitution sites for both HB-MTW and HAl-MTW zeolites, while the DFT show that T(1) and T(3) are the most favored sites for HB-MTW and HAl-MTW zeolites, respectively. For HGa-MTW, the DFT-D2 results indicates that the favored Ga location following the order: T(4) > T(3) > T(5) > T(6) > T(1) = T(2) > T(7), v.s. the DFT results of: T(4) > T(3) > T(5) > T(1) > T(6) > T(7) > T(2).

(Table 2)

(Table 3)

The computed adsorption energies (Table 3) show that the DFT obviously underestimates the adsorption energies for the adsorption of NH_3 and pyridine in the zeolites, compared with the DFT-D2 methods. Table 4 shows that DFT also underestimated the substitution energies almost more than 1.00 eV for the B, Al and Ga incorporated MTW zeolites compared to DFT-D2 method. These results indicate that the dispersion correction is essential for zeolite system and should be taken into account when calculating adsorption energies and substitution energies.

(Table 4)

3.1 Structures

3.1.1 B-MTW. Figure 2 shows the most stable local structures for each location and relative energies for HB-MTW, LiB-MTW, NaB-MTW and KB-MTW zeolites. (The more detailed local minima structures and relative energies for HB-MTW, LiB-MTW, NaB-MTW and KB-MTW zeolites are shown in Figure **S1-S4** of the **Supplementary Materials**). It is found that the most favored B locations are T(4), T(7) and T(3) sites for HB-MTW, LiB-MTW, NaB-MTW and KB-MTW zeolites, respectively. For HB-MTW, the energy differences for B in different T sites are less than 0.21 eV. Such small energy difference indicates that B atom could distribute in all T sites of the zeolites when HB-MTW were synthesized. While, for LiB-MTW, NaB-MTW and KB-MTW zeolites, the energies of T(3), T(5) and T(7) sites are 0.64, 0.55 and 0.69 eV larger than that of associated most favorable T(4), T(7) and T(3) sites, respectively. Unlike HB-MTW, the B atom of LiB-MTW, NaB-MTW and KB-MTW should selectively distribute in some specific T sites instead of all T sites due to the larger energy differences.

(Figure 2)

3.1.2 Al-MTW. Figure 3 shows the most stable local structures for Al locations and relative energies of HAl-MTW, LiAl-MTW, NaAl-MTW and KAl-MTW zeolites. (The more detailed local minima structures and relative energies for HAl-MTW, LiAl-MTW, NaAl-MTW and KAl-MTW zeolites are shown in Figure **S5-S8** in **Supplementary Materials**). The results show that the most stable Al locations for the HAl-MTW, LiAl-MTW, NaAl-MTW and KAl-MTW zeolites are T(4), T(5) T(5) and T(3) sites, respectively. It is interesting to note that the energy differences for Al in different T sites of the MTW zeolite are small (less than 0.30 eV), which indicates Al could distribute in all T sites of H-, Li-, Na- and K-forms of MTW zeolites.[38] This result agrees well with the experiment results, in which Smirniotis et al observed that the Al atoms can distribute in various T sites of the synthesized NaAl-MTW.[49]

(Figure 3)

3.1.3 Ga-MTW. Figure 4 shows the most stable local structures for Ga locations and relative energies of HGa-MTW, LiGa-MTW, NaGa-MTW and KGa-MTW zeolites. (The more detailed local minima structures and relative energies for HGa-MTW, LiGa-MTW, NaGa-MTW and KGa-MTW zeolites are shown in Figure **S9-S12** in **Supplementary Materials**). The results show that the most stable Ga locations for the HGa-MTW, LiGa-MTW, NaGa-MTW and KGa-MTW zeolites are T(4), T(7) T(4) and T(5) sites, respectively. The energy differences for Ga in different T sites of the HGa-MTW, LiGa-MTW, NaGa-MTW and KGa-MTW zeolites are 0.18, 0.28, 0.43 and 0.35 eV, respectively.

(Figure 4)

It is interesting to note that the T(4) site is always the most stable site for B, Al and Ga incorporated H-form form MTW zeolites. Our results also indicates that the locations of Al in the MTW zeolites may be different from those of B and Ga for Li-, Na- and K-forms of MTW zeolites, since the energy differences for B and Ga in different T sites of the Li-, Na- and K-forms of MTW zeolites are large. It indicates that the alkaline metal ions may influence the locations of the trivalent B and Ga in the zeolites. Especially for B-MTW, the energy differences for B in different T sites of LiB-MTW, NaB-MTW and KB-MTW zeolites are 0.64, 0.55 and 0.69 eV, respectively. To the best of our knowledge, no experimental works have been reported on controlling the locations of trivalent B and Ga in the MTW zeolites using different alkaline metal ions. Our calculation results provided a new option to selectively synthesize specific T sites substituted B-MTW zeolite using Li, Na and K as the alkaline metal ions, which need to be confirmed by experiments.

In addition, our results show that the H, Li and Na atoms could stay in both the main channels and the cages of the zeolites. In contrast, the K could only stay in the main channel of the zeolites. This is probably because that the size of K is larger than that of H, Li and Na,[50]

and the cages of the zeolites are too small to hold the K.

3.1.4 Cell volume and bond distance.

Volume change is also essential for the relative stability as reported before.[51,52] In order to study the influence caused by the volume changes, we followed the references and calculated the energies for the stable H-form B, Al, Ga incorporated and pure silica MTW zeolites with variable volumes, which were plotted in Figure 5. For each type zeolite, a quadratic equation was fitted to describe the associated parabolic curve. The results show that the equilibrium volumes of the *p*(1×2×1) HB-MTW, HAl-MTW, HGa-MTW and pure silica MTW cell are 3018.24, 3046.41, 3044.02 3173.39 $Å^3$, respectively, which are in well agreement with our direct optimized results.

(Figure 5)

The bond distances and *p*(1×2×1) cell volumes of the MTW zeolites before and after the substitution of Si by B, Al and Ga are shown in Table 5. It should be noted that the cell volume of pure silica MTW zeolite is 3173.39 $Å^3$, with Si–O bond distances in the range of 1.61~1.63 Å. As shown in Table 4 and Figure 2-4, the O–H bond distances are in the range of 0.98~0.99, 0.99~1.03 and 0.99~1.03 Å, respectively for HB-MTW, HAl-MTW and HGa-MTW zeolites, which are similar to the calculated O–H bond in H_2O molecule (0.99 Å), H-form Al-BEA (0.982~1.002 Å, VWN functional)[53] and H-form Al-MOR (0.991~1.000 Å, PW91 functional)[52]. The shorter H–O bond distances of HB-MTW indicates the weaker Brønsted acidity of HB-MTW comparing to that of HAl-MTW and HGa-MTW. The distances from the alkaline metal to its nearest O atoms follow the order of Li–O < Na–O < K–O. The Li–O bond distances are in the range of 1.92~2.06 Å, 1.89~2.15 Å and 1.87~2.03 Å for the B, Al and Ga incorporated MTW zeolites, respectively. In comparison, the Na–O bond distances are in the range of 2.25~2.44 Å, 2.24~2.45 Å and 2.20~2.28 Å and the K–O bond distances are in the range of 2.62~2.92 Å, 2.63~2.81 Å and 2.61~2.70 Å, respectively. It is interesting

to note that the Li–O, Na–O and K–O bond distances of the Ga-MTW zeolites are shorter than in the B-MTW and Al-MTW zeolites.

(Table 5)

As the atomic covalent radius increase for B, Al and Ga (0.82, 1.18 and 1.26 Å, respectively),[50] the related M–O (M = B, Al, Ga) bond distances and cell volumes of the zeolites also increases monotonically. For the HB-MTW, three B–O bond distances are in the ranges of 1.37~1.39 Å, while the other one is 2.61~2.89 Å, which indi cates that the B atoms are three-fold coordinated in the HB-MTW. It was also found that the BO_3 species are almost coplanar (Figure 2). While the B–O bond distances are in the ranges of 1.43~1.54 Å, 1.44~1.51 Å and 1.45~1.51 Å for LiB-MTW, NaB-MTW and KB-MTW zeolites, respectively, which indicates the B atoms are tetra-coordinated. Similar cases were also found for Al and Ga incorporated H-form MTW zeolites. As shown in Table 4 and Figure 3-4, although Ga and Al are still tetra-coordinated in the T sites of HAl-MTW and HGa-MTW zeolites, one of the Ga–O and Al–O bonds are obviously elongated compared with the other three Ga–O and Al–O bonds, since the O–H bonds weakened the related Ga–O and Al–O bonds.

The bond distances also influence the cell volumes of the zeolites. Since the B–O bond distances are obviously shorter than the Si–O bonds, the cell volumes of B-MTW zeolites are smaller that pure silica MTW zeolite. It agrees well with the reported experiments that the cell volume decreases as the B content increases in the zeolites.[32] The $p(1\times2\times1)$ cell volume of the LiB-MTW zeolite are in the ranges of 2946.81~2999.82 $Å^3$ in comparison to that of 2975.79~3130.93 $Å^3$ and 2992.63~3137.90 $Å^3$ for NaB-MTW and KB-MTW zeolites, respectively. Since one of the B–O distances is elongated to 2.61~2.89 Å, the $p(1\times2\times1)$ cell volumes of the HB-MTW is in the range of 3018.24~3071.33 $Å^3$, which is significantly larger than the cell volumes of LiB-MTW. It was also found that the cell volumes of H-forms Al and Ga incorporated MTW zeolites are larger than those of Li-form MTW zeolites. The cell

volumes of Na-form Al and Ga incorporated MTW zeolites are comparable with H-form zeolites, while smaller than those of K-form zeoltes.

3.1.5 Charge density. In order to map out the bond properties for B, Al and Ga incorporated MTW zeolites, the electron density for the T sites of MTW zeolite after B, Al and Ga substitution were plotted using VESTA.[54,55] Figure 6 show that the B–O, Si–O and O–H bonds are obvious covalent bonds. While the Na–O and Al–O bonds show obvious ionic property. The Ga–O bond shows the property in the between of covalent bonds and ionic bond.

(Figure 6)

3.2 Substitution energy

The calculated substitution energies are shown in Table 3. It should be noted that we focus on the Li, Na, K ect. cation themselves without solvation effect. It shows that the substitution energies for the B-MTW zeolites follow the order: HB-MTW (0.20~0.41 eV) < NH_4B-MTW (–0.05~–0.62 eV) < NaB-MTW (–2.07~–2.62 eV) ≈ KB-MTW (–2.04~–2.74 eV) < LiB-MTW (–2.90~–3.53 eV). It indicates that Li should be the most thermodynamically favored alkaline ion for the synthesis of B-MTW zeolite.

The substitution energies for the H-form B-MTW zeolite are positive, which indicates synthesis reaction of HB-MTW is thermodynamically not favored. The substitution energies for the NH_4-form B-MTW zeolite is slightly negative, which indicates the synthesis of NH_4B-MTW may be attainable, while the driving force for NH_4B-MTW zeolites synthesis reactions are much less than the reactions for Li-, Na- and K-form MTW zeolites. From the thermodynamics point of view, the K and Na may contribute similar effects to the B-MTW zeolites synthesis, since the substitution energies of NaB-MTW are closed to those of the KB-MTW zeolites.

Similar to the case of B-MTW, the substitution energies of Al and Ga incorporated MTW zeolites also follow the order that H-form < NH_4-form < Na-form ≈ K-form < Li-form. It should be noted that the substitution energies of Al-MTW are larger than those of Ga-MTW and B-MTW, which indicates that for each form of MTW zeolites, the Al-MTW could be synthesized more easily, followed by Ga-MTW and B-MTW. Yuan et al. calculated the substitution of Si by B, Al and Ga for mordeinte cluster using Hartree-Fock MO methods,[34] they also found that the substitution are favored following the order of Al > Ga > B. LiAl-MTW zeolites have the largest substitution energies, indicating that Al and Li are the most favored trivalent and alkaline metal for the synthesis of MTW-type zeolites. It should be noted that Li is always a better alkaline metal ion than Na and K for the synthesis of B, Al and Ga incorporated MTW zeolites, since the substitution energies of Li-form MTW are larger than those of H-, NH_4-, Na- and K-form MTW zeolites. Okubo et al investigated the synthesis of Al-MTW,[29] and found that Li indeed worked better Na. Although we failed to find the experimental work reported on the synthesis of LiB-MTW and LiGa-MTW, our calculated results provided useful information for experimentalists.

Direct synthesis of NH_4-form and H-form zeolites without alkali metal cations can be advantageous over conventional methods by eliminating the ion-exchange steps.[56] It should be noted that the substitution energies of NaB-MTW is similar to those of NH_4Al-MTW and NH_4Ga-MTW. NaB-MTW zeolites had been successfully synthesized.[30] It indicates that direct synthesis of NH_4-form Al and Ga incorporated MTW zeolites is possible under proper conditions.[24] The positive substitution energies of HB-MTW indicating the synthesis reaction of the HB-MTW is thermodynamically unfavorable. Direct synthesis of Ga and Al incorporated H-form MTW zeolites seems thermodynamically favorable, as indicated by the calculated substitution energies. While the driving force for H-form zeolites synthesis reactions are much less than the reactions for Li, Na, K, and NH_4-form zeolites synthesis.

Furthermore, it was found that the most favored substitution sites for B, Al and Ga are different as the type of alkaline ion changes, i.e. the T(4) site is the most favored substitution sites for HB-MTW and LiB-MTW whereas T(2), T(7) and T(3) are the most favored substitution sites for NH_4B-MTW, NaB-MTW and KB-MTW zeolites. It indicates that the alkaline metal ions may influence the location of the trivalent B, Al and Ga atom in the MTW-type zeolites.

3.3 Acid Property

Figure 7 shows the local structures with the largest adsorption energies for the adsorption of NH_3 and pyridine on both Lewis and Brønsted acid sites in HB-MTW, HAl-MTW and HGa-MTW zeolites. (The more detailed adsorption energies and structures are shown in **Table 2** and **Figure S13-S18** in **Supplementary Materials**.) It shows that the adsorption energies for pyridine are larger than that for NH_3 in both Lewis and Brønsted acid sites of the zeolites. For example, the adsorption energies for NH_3 in Lewis and Brønsted acid sites of HB-MTW, HAl-MTW and HGa-MTW are –1.03 eV, –1.10 eV, –1.18 eV and –1.28 eV, –1.69 eV, –1.58 eV, respectively. In comparison, the adsorption energies for pyridine in Lewis and Brønsted acid sites are –1.43 eV, –1.43 eV, –1.61 eV and –1.90 eV, –2.26 eV, –2.10 eV, respectively. Furthermore, we calculated the adsorption of NH_3 molecule in the cages of the zeolite, i.e. in **B(1)-H-NH_3-2**, the adsorption energies are less exothermic by 0.52 eV than in the main channel of the zeolite **B(1)-H-NH_3-3** in **Fig S13**. This result is similar to the cases for NH_3 adsorption in the HAl-MTW and HFe-MTW zeolites.[38,39] It indicates the NH_3 molecules are more favored in the main channel than in the small cages of the zeolites, since the cages of the zeolites are not large enough to hold the NH_3 molecule.

It was found that the NH_3 and pyridine could react with the proton of Brønsted acid sites of the zeolites and form NH_4 and C_5NH_6 species. As indicated by the calculated adsorption energies, the adsorption of NH_3 and pyridine on Brønsted acid sites is stronger than on Lewis

acid sites. The Brønsted acid sites of the zeolites follow order: HB-MTW < HGa-MTW < HAl-MTW. These results agree well with the reported NH_3-TPD experiments that the acid strength of the HGa-MTW is less than the HAl-MTW,[31] and the present results for the MTW zeolites are similar to the reported experimental and computational results on the MFI and MOR zeolites that the acidities of the B incorporated zeolites are weaker than the Ga and Al incorporated zeolites.[34,35,57-59] In addition, the Lewis acidity of HB-MTW is similar to that of HAl-MTW, while weaker than the HGa-MTW.

(Figure 7)

4. Conclusions

The B, Ga and Al incorporated MTW-type zeolites were systematically studied using dispersion-corrected periodic DFT. Our computational results show that dispersion correction is very important for such zeolites systems, since DFT underestimates the adsorption energies for NH_3 and pyridine. DFT also underestimated the substitution energies more than 1.00 eV for the B, Ga and Al incorporated MTW zeolites compared to DFT-D2 method.

In the HB-MTW zeolites, the B atoms are three-fold coordinated, while in the LiB-MTW, NaB-MTW and KB-MTW zeolites, the B atoms are tetra-coordinated. The Al and Ga in the H-, NH_4-, Li-, Na- and K-forms MTW zeolites are tetra-coordinated. The K was found to stay only in the main channel of the zeolites, while H, Li and Na were found possible to stay in both the small cages and the main channel of the zeolites. Charge density analysis shows that the B–O, Si–O and O–H bonds are obvious covalent bonds while the Na–O and Al–O bonds show obvious ionic property. In addition, the Ga–O bonds show the property between the Al–O and B–O bonds. The cell volumes were found to be sensitive to alkaline metal ions. H-form B, Al and Ga incorporated MTW zeolites were found have larger cell volumes than Li-form MTW zeolites, while smaller than K-form MTW zeolites.

For the synthesis prescriptions of the MTW zeolites, the trivalent and alkaline metal ions

were found be favored following the order: Al > Ga > B, Li > K ≈ Na > NH_4 > H. The Li, Na and K ions could influence the location of B and Ga atoms in the zeolites.

As indicated by the adsorption energies of NH_3 and pyridine in the zeolite, the adsorption of pyridine is much stronger than NH_3 adsorption. The Brønsted acid sites of the zeolites follow the order of HB-MTW < HGa-MTW < HAl-MTW. The Lewis acidity of HB-MTW is similar to that of HAl-MTW, while weaker than the HGa-MTW. These results are in well agreement with the previous experiments and provide new insight for the MTW zeolite.

Acknowledgements

This work is supported by SINOPEC, the China Petroleum and Chemical Corporation, and Shenzhen Strategic Emerging Industries Special Fund Program of China (Grant No. GGJS20120619101655715 and JCY20120619101655719).

Appendix A. Supplementary data

Supplementary data associated with this article can be found, in the online version, at http://dx.doi.org/

Table 1 Cutoff energy (350~1000 eV) influence for the H-form Al-MTW zeolite. The adsorption energy of NH_3 (E_{ads}, eV) and substitution energy (E_{sub} eV) were tested. Both of the ion positions and cell parameters were fully relaxed in the calculations.

HAl-MTW	ENCUT (eV)	350	400	500	600	700	800	900	1000
Al(1)	E_{sub}	–1.65	–1.64	–1.63	–1.63	–1.66	–1.67	–1.67	–1.67
	E_{ads} (NH_3)	–1.62	–1.62	–1.61	–1.66	–1.63	–1.62	–1.63	–1.63
Al(2)	E_{sub}	–1.60	–1.59	–1.57	–1.57	–1.56	–1.57	–1.63	–1.58
	E_{ads} (NH_3)	–1.54	–1.53	–1.53	–1.62	–1.63	–1.65	–1.58	–1.63
Al(3)	E_{sub}	–1.72	–1.71	–1.69	–1.74	–1.75	–1.74	–1.74	–1.75
	E_{ads} (NH_3)	–1.66	–1.66	–1.66	–1.68	–1.66	–1.68	–1.69	–1.68
Al(4)	E_{sub}	–1.82	–1.81	–1.79	–1.85	–1.85	–1.85	–1.87	–1.86
	E_{ads} (NH_3)	–1.36	–1.36	–1.36	–1.39	–1.39	–1.40	–1.38	–1.39
Al(5)	E_{sub}	–1.67	–1.66	–1.64	–1.71	–1.72	–1.72	–1.72	–1.72
	E_{ads} (NH_3)	–1.43	–1.42	–1.42	–1.41	–1.41	–1.41	–1.41	–1.41
Al(6)	E_{sub}	–1.66	–1.65	–1.63	–1.68	–1.69	–1.70	–1.69	–1.70
	E_{ads} (NH_3)	–1.69	–1.68	–1.68	–1.70	–1.70	–1.70	–1.70	–1.69
Al(7)	E_{sub}	–1.70	–1.70	–1.68	–1.75	–1.75	–1.76	–1.76	–1.76
	E_{ads} (NH_3)	–1.51	–1.50	–1.50	–1.47	–1.47	–1.45	–1.46	–1.47

Table 2 Relative energies (eV) for B, Al and Ga incorporated H-form MTW zeolite calculated with DFT-D2 (*ΔE* (DFT-D2)), DFT (*ΔE* (DFT)) and dispersion correction (*ΔE*(D2)), respectively. The relative energies of the other structures are given with respective to the most stable structure.

Structure	*ΔE*(DFT-D2)	*ΔE*(DFT)	*ΔE*(D2)	Structure	*ΔE*(DFT-D2)	*ΔE*(DFT)	*ΔE*(D2)
B(1)-H-1	0.96	0.27	0.69	Al(5)-H-2	0.16	0.13	0.02
B(1)-H-2	0.25	0.23	0.02	Al(5)-H-3	0.29	0.32	–0.04
B(1)-H-3	0.54	–0.15	0.68	Al(6)-H-1	0.27	0.24	0.03
B(1)-H-4	0.11	0.06	0.05	Al(6)-H-2	0.17	0.31	–0.14
B(1)-H-5	0.69	–0.07	0.76	Al(6)-H-3	0.17	0.20	–0.03
B(2)-H-1	0.09	0.04	0.05	Al(6)-H-4	0.64	0.68	–0.04
B(2)-H-2	0.55	–0.02	0.58	Al(7)-H-1	0.36	0.29	0.06
B(2)-H-3	0.19	0.27	–0.08	Al(7)-H-2	0.37	0.43	–0.06
B(2)-H-4	0.37	0.25	0.12	Al(7)-H-3	0.12	0.25	–0.13
B(3)-H-1	0.67	0.08	0.59	Al(7)-H-4	0.15	0.14	0.00
B(3)-H-2	0.87	0.22	0.65	Ga(1)-H-1	0.19	0.16	0.03
B(3)-H-3	0.12	0.14	–0.02	Ga(1)-H-2	0.49	0.69	–0.21
B(3)-H-4	0.09	0.09	0.00	Ga(1)-H-3	0.16	0.24	–0.08
B(4)-H-1	0.73	–0.02	0.75	Ga(1)-H-4	0.26	0.26	0.00
B(4)-H-2	0.74	0.20	0.55	Ga(2)-H-1	0.16	0.32	–0.16
B(4)-H-3	**0.00**	**0.00**	**0.00**	Ga(2)-H-2	0.20	0.33	–0.13
B(4)-H-4	0.64	–0.09	0.73	Ga(2)-H-3	0.27	0.32	–0.05
B(5)-H-1	0.05	–0.02	0.07	Ga(2)-H-4	0.17	0.45	–0.29
B(5)-H-2	0.16	0.15	0.01	Ga(2)-H-5	0.20	0.32	–0.12
B(5)-H-3	0.66	0.09	0.56	Ga(3)-H-1	0.09	0.03	0.06
B(5)-H-4	0.24	0.15	0.08	Ga(3)-H-2	0.14	0.39	–0.25
B(6)-H-1	0.62	–0.02	0.63	Ga(3)-H-3	0.29	0.52	–0.23
B(6)-H-2	0.21	–0.07	0.28	Ga(3)-H-4	0.09	0.09	0.00
B(6)-H-3	0.97	0.28	0.69	Ga(4)-H-1	0.16	0.21	–0.05
B(6)-H-4	0.83	0.04	0.79	Ga(4)-H-2	0.36	0.23	0.13
B(6)-H-5	0.56	–0.05	0.61	Ga(4)-H-3	0.31	0.45	–0.14
B(7)-H-1	1.93	1.26	0.67	**Ga(4)-H-4**	**0.00**	**0.00**	**0.00**
B(7)-H-2	0.20	0.15	0.06	Ga(5)-H-1	0.27	0.30	–0.03
B(7)-H-3	0.73	–0.03	0.76	Ga(5)-H-2	0.41	0.51	–0.10
B(7)-H-4	0.84	0.20	0.65	Ga(5)-H-3	0.10	0.16	–0.06
B(7)-H-5	0.47	–0.12	0.59	Ga(5)-H-4	0.36	0.41	–0.04
B(7)-H-6	0.87	0.14	0.72	Ga(5)-H-5	0.10	0.04	0.05
Al(1)-H-1	0.17	0.00	0.17	Ga(6)-H-1	0.20	0.38	–0.18
Al(1)-H-2	0.97	0.30	0.66	Ga(6)-H-2	0.13	0.21	–0.08
Al(2)-H-1	0.22	0.20	0.02	Ga(6)-H-3	0.22	0.18	0.03
Al(2)-H-2	0.22	0.35	–0.12	Ga(6)-H-4	0.53	0.54	–0.01
Al(2)-H-3	0.22	0.22	0.00	Ga(6)-H-5	0.54	0.58	–0.04
Al(3)-H-1	0.10	–0.01	0.12	Ga(6)-H-6	0.20	0.39	–0.19
Al(3)-H-2	0.25	0.35	–0.09	Ga(7)-H-1	0.21	0.31	–0.10
Al(3)-H-3	0.31	0.49	–0.18	Ga(7)-H-2	0.21	0.23	–0.02
Al(4)-H-1	0.16	0.07	0.09	Ga(7)-H-3	0.31	0.41	–0.11
Al(4)-H-2	0.24	0.12	0.12	Ga(7)-H-4	0.35	0.52	–0.17
Al(4)-H-3	0.40	0.53	–0.13	Ga(7)-H-5	0.24	0.43	–0.19
Al(4)-H-4	**0.00**	**0.00**	**0.00**	Ga(7)-H-6	0.18	0.21	–0.02
Al(5)-H-1	0.27	0.23	0.04				

Table 3 Adsorption energies (E_{ads}, eV) for the adsorption of NH_3 and pyridine on both the Brønsted (B) and Lewis (L) acid sites in B, Al and Ga incorporated H-form MTW zeolite calculated with DFT-D2 and DFT, respectively.

Structures	E_{ads}(DFT-D2)	E_{ads}(DFT)	Structures	E_{ads}(DFT-D2)	E_{ads}(DFT)
B(1)-H-NH_3-1(L)	–1.03	–0.62	Ga(5)-H-NH_3-3(B)	–1.35	–0.98
B(1)-H-NH_3-2(B)	–0.57	0.06	Ga(6)-H-NH_3-1(L)	–0.36	–0.04
B(1)-H-NH_3-3(B)	–1.09	–0.69	Ga(6)-H-NH_3-2(B)	–1.49	–1.29
B(2)-H-NH_3-1(B)	–1.28	–0.69	Ga(6)-H-NH_3-3(B)	–1.20	–0.64
B(2)-H-NH_3-2(L)	–0.30	0.36	Ga(6)-H-NH_3-4(B)	–0.65	–0.23
B(3)-H-NH_3-1(L)	–1.00	–0.61	Ga(7)-H-NH_3-1(B)	–1.48	–1.17
B(3)-H-NH_3-2(B)	–0.79	–0.37	B(1)-H-Py-1(L)	–1.43	–0.55
B(3)-H-NH_3-3(B)	–1.25	–0.73	B(1)-H-Py-2(B)	–1.75	–0.64
B(4)-H-NH_3-1(L)	–0.99	–0.53	B(2)-H-Py-1(L)	–1.27	–0.38
B(4)-H-NH_3-2(B)	–0.64	–0.25	B(2)-H-Py-2(B)	–1.86	–0.78
B(4)-H-NH_3-3(B)	–1.02	–0.71	B(3)-H-Py-1(L)	–1.38	–0.47
B(5)-H-NH_3-1(B)	–0.81	–0.49	B(3)-H-Py-2(B)	–0.59	0.43
B(5)-H-NH_3-2(L)	–0.53	–0.05	B(3)-H-Py-3(B)	–1.27	–0.23
B(5)-H-NH_3-3(B)	–1.02	–0.58	B(4)-H-Py-1(L)	–1.31	–0.34
B(6)-H-NH_3-1(B)	–0.95	–0.50	B(4)-H-Py-2(B)	–1.60	–0.63
B(6)-H-NH_3-2(L)	–0.66	–0.03	B(5)-H-Py-1(B)	–1.17	–0.36
B(7)-H-NH_3-1(B)	–0.83	–0.49	B(5)-H-Py-2(L)	–0.45	0.54
Al(1)-H-NH_3-1(L)	–0.34	0.11	B(6)-H-Py-1(B)	–1.26	–0.40
Al(1)-H-NH_3-2(L)	–0.85	–0.31	B(6)-H-Py-2(B)	–1.90	–0.78
Al(1)-H-NH_3-3(B)	–1.62	–1.34	B(6)-H-Py-3(L)	–0.51	0.34
Al(2)-H-NH_3-1(L)	–1.06	–0.71	B(7)-H-Py-1(B)	–0.51	0.45
Al(2)-H-NH_3-2(B)	–1.53	–1.20	B(7)-H-Py-2(B)	–1.25	–0.30
Al(3)-H-NH_3-1(B)	–1.66	–1.23	Al(1)-H-Py-1(B)	–2.26	–1.45
Al(3)-H-NH_3-2(L)	–0.54	–0.05	Al(1)-H-Py-2(L)	–0.72	0.18
Al(4)-H-NH_3-1(L)	–1.10	–0.76	Al(2)-H-Py-1(L)	–1.40	–0.68
Al(4)-H-NH_3-2(B)	–0.73	–0.23	Al(2)-H-Py-2(B)	–2.08	–1.34
Al(4)-H-NH_3-3(B)	–1.36	–1.09	Al(3)-H-Py(B)	–2.09	–1.26
Al(5)-H-NH_3-1(L)	–1.07	–0.75	Al(4)-H-Py-1(L)	–1.31	–0.32
Al(5)-H-NH_3-2(B)	–0.88	–0.56	Al(4)-H-Py-2(B)	–1.55	–0.66
Al(5)-H-NH_3-3(B)	–1.43	–1.30	Al(5)-H-Py-1(L)	–1.37	–0.68
Al(6)-H-NH_3-1(L)	–0.97	–0.76	Al(5)-H-Py-2(B)	–2.14	–1.38
Al(6)-H-NH_3-2(B)	–1.17	–0.68	Al(6)-H-Py-1(L)	–1.43	–0.64
Al(6)-H-NH_3-3(B)	–1.69	–1.31	Al(6)-H-Py-2(B)	–2.11	–1.51
Al(7)-H-NH_3-1(B)	–1.51	–1.31	Al(7)-H-Py(B)	–1.74	–1.09
Al(7)-H-NH_3-2(B)	–0.91	–0.53	Ga(1)-H-Py-1(L)	–0.76	0.05
Ga(1)-H-NH_3-1(B)	–1.50	–1.21	Ga(1)-H-Py-2(B)	–2.10	–1.23
Ga(1)-H-NH_3-2(L)	–0.46	–0.12	Ga(2)-H-Py-1(L)	–1.05	–0.21
Ga(1)-H-NH_3-3(L)	–0.83	–0.39	Ga(2)-H-Py-2(B)	–2.07	–1.36
Ga(1)-H-NH_3-4(B)	–1.09	–0.49	Ga(3)-H-Py-1(B)	–1.82	–1.16
Ga(2)-H-NH_3-1(B)	–1.54	–1.28	Ga(3)-H-Py-2(L)	–0.76	0.15
Ga(2)-H-NH_3-2(L)	–0.64	–0.22	Ga(4)-H-Py-1(L)	–1.61	–0.64
Ga(3)-H-NH_3-1(B)	–1.58	–1.21	Ga(4)-H-Py-2(B)	–1.92	–1.07
Ga(3)-H-NH_3-2(L)	–0.82	–0.26	Ga(5)-H-Py-1(L)	–1.50	–0.67
Ga(4)-H-NH_3-1(L)	–1.18	–0.78	Ga(5)-H-Py-2(B)	–1.94	–1.04
Ga(4)-H-NH_3-2(B)	–0.52	–0.17	Ga(6)-H-Py-1(L)	–0.67	0.08
Ga(4)-H-NH_3-3(B)	–1.39	–0.93	Ga(6)-H-Py-2(B)	–2.02	–1.27
Ga(5)-H-NH_3-1(B)	–1.10	–0.75	Ga(7)-H-Py-1(B)	–1.65	–0.68
Ga(5)-H-NH_3-2(L)	–0.74	–0.25			

a) The adsorption energies for NH_3 and pyridine in HAl-MTW were from ref.

Table 4 Substitution energies (E_{sub}, eV) for the substitution of one Si atom with M (M = B, Al, Ga) and Y (Y = NH_4, Li, Na, K, H) in MTW-type zeolite calculated with DFT-D2 (and DFT).

Substitution sites	T(1)	T(2)	T(3)	T(4)	T(5)	T(6)	T(7)
H-B	0.31 (1.15)	0.29 (1.13)	0.30 (1.19)	0.20 (1.09)	0.26 (1.08)	0.42 (1.03)	0.41 (1.24)
NH_4-B	–0.40 (0.80)	–0.62 (0.79)	–0.57 (0.79)	–0.44 (0.73)	–0.39 (0.84)	–0.16 (0.87)	–0.05 (1.10)
Li-B	–3.18 (–1.73)	–3.15 (–1.53)	–2.90 (–1.42)	–3.53 (–1.73)	–3.48 (–1.81)	–3.33 (–1.75)	–3.33 (–1.87)
Na-B	–2.59 (–1.24)	–2.37 (–0.75)	–2.56 (–1.08)	–2.52 (–0.74)	–2.07 (–1.34)	–2.55 (–1.08)	–2.62 (–1.13)
K-B	–2.71 (–1.47)	–2.23 (–1.61)	–2.74 (–1.49)	–2.20 (–1.57)	–2.15 (–1.63)	–2.57 (–1.30)	–2.04 (–1.28)
H-Al	–1.65 (–0.96)	–1.61 (–0.74)	–1.72 (–0.97)	–1.82 (–0.96)	–1.67 (–0.83)	–1.66 (–0.65)	–1.70 (–0.71)
NH_4-Al	–2.90 (–1.97)	–2.76 (–1.62)	–3.01 (–1.86)	–2.80 (–1.70)	–2.72 (–1.79)	–2.96 (–1.72)	–2.83 (–1.78)
Li-Al	–5.56 (–4.11)	–5.58 (–3.86)	–5.50 (–4.12)	–5.57 (–4.12)	–5.70 (–4.02)	–5.55 (–4.24)	–5.69 (–4.17)
Na-Al	–4.89 (–3.68)	–4.85 (–3.56)	–4.99 (–3.61)	–4.92 (–3.74)	–5.08 (–3.64)	–4.91 (–3.46)	–5.02 (–3.54)
K-Al	–4.92 (–3.82)	–5.06 (–3.61)	–5.12 (–3.81)	–5.04 (–3.78)	–4.92 (–3.71)	–5.02 (–3.83)	–4.81 (–3.45)
H-Ga	–0.98 (0.07)	–0.97 (0.16)	–1.05 (–0.14)	–1.13 (–0.17)	–1.04 (–0.12)	–1.00 (0.05)	–0.95 (0.04)
NH_4-Ga	–2.10 (–0.79)	–2.13 (–0.78)	–2.24 (–1.01)	–2.14 (–0.76)	–2.01 (–0.76)	–2.11 (–0.91)	–2.05 (–0.78)
Li-Ga	–4.96 (–3.57)	–4.84 (–3.30)	–4.78 (–3.14)	–4.84 (–3.00)	–5.02 (–3.19)	–4.89 (–3.34)	–5.06 (–3.31)
Na-Ga	–4.15 (–2.60)	–4.11 (–2.63)	–4.21 (–2.72)	–4.48 (–3.03)	–4.05 (–2.67)	–4.20 (–2.47)	–4.30 (–2.46)
K-Ga	–4.24 (–2.83)	–4.23 (–2.72)	–4.39 (–3.02)	–4.37 (–2.97)	–4.41 (–3.20)	–4.18 (–3.00)	–4.06 (–2.62)

Table 5 Bond distances and *p*(1×2×1) cell volumes of the B, Al and Ga incorporated MTW zeolite.

T sites		T1	T2	T3	T4	T5	T6	T7
T–O (Å)	Si	1.62,1.62, 1.62,1.63	1.62,1.62, 1.63,1.63	1.61,1.62, 1.62,1.63	1.61,1.62, 1.62,1.63	1.62,1.62, 1.62,1.63	1.62,1.62, 1.62,1.63	1.62,1.62, 1.62,1.62
	HB	1.38,1.38, 1.39,2.61	1.37,1.38, 1.39,2.72	1.37,1.38, 1.39,2.85	1.37,1.39, 1.39,2.89	1.37,1.37, 1.38,2.82	1.37,1.38, 1.38,2.63	1.38,1.38, 1.38,2.77
	LiB	1.45,1.46, 1.50,1.52	1.44,1.45, 1.51,1.52	1.45,1.45, 1.50,1.51	1.43,1.46, 1.51,1.54	1.43,1.46, 1.51,1.53	1.43,1.47, 1.50,1.54	1.43,1.47, 1.51,1.51
	NaB	1.45,1.46, 1.49,1.50	1.45,1.48, 1.49,1.50	1.44,1.49, 1.49,1.51	1.45,1.46, 1.51,1.51	1.44,1.44, 1.52,1.52	1.45,1.46, 1.49,1.51	1.44,1.49, 1.49,1.50
	KB	1.45,1.47, 1.49,1.50	1.45,1.47, 1.50,1.50	1.45,1.48, 1.49,1.50	1.45,1.47, 1.49,1.50	1.44,1.46, 1.51,1.51	1.45,1.47, 1.50,1.50	1.45,1.47, 1.50,1.50
	HAl	1.71,1.72, 1.72,1.89	1.71,1.72, 1.72,1.89	1.71,1.72, 1.72,1.91	1.71,1.72, 1.74,1.89	1.72,1.72, 1.73,1.92	1.71,1.72, 1.72,1.90	1.71,1.72, 1.72,1.88
	LiAl	1.72,1.73, 1.75,1.78	1.71,1.73, 1.76,1.78	1.72,1.74, 1.75,1.81	1.72,1.72, 1.77,1.79	1.72,1.74, 1.74,1.81	1.72,1.74, 1.76,1.79	1.72,1.74, 1.77,1.78
	NaAl	1.72,1.73, 1.75,1.77	1.73,1.73, 1.77,1.78	1.72,1.73, 1.77,1.78	1.73,1.73, 1.77,1.78	1.73,1.75, 1.77,1.78	1.73,1.75, 1.75,1.78	1.71,1.74, 1.76,1.77
	KAl	1.73,1.73, 1.76,1.77	1.73,1.73, 1.76,1.77	1.72,1.74, 1.77,1.77	1.72,1.74, 1.76,1.77	1.73,1.73, 1.77,1.77	1.73,1.73, 1.75,1.77	1.73,1.73, 1.75,1.78
	HGa	1.79,1.79, 1.79,2.01	1.79,1.79, 1.80,2.03	1.79,1.79, 1.79,2.04	1.78,1.79, 1.81,2.03	1.79,1.79, 1.81,2.05	1.79,1.79, 1.79,2.01	1.79,1.79, 1.80,2.02
	LiGa	1.80,1.80, 1.86,1.87	1.79,1.80, 1.87,1.87	1.80,1.81, 1.85,1.88	1.78,1.83, 1.83,1.88	1.80,1.82, 1.82,1.91	1.78,1.82, 1.86,1.90	1.79,1.81, 1.86,1.87
	NaGa	1.80,1.82, 1.85,1.85	1.81,1.81, 1.86,1.86	1.80,1.83, 1.85,1.87	1.80,1.80, 1.86,1.87	1.79,1.81, 1.85,1.88	1.79,1.82, 1.86,1.87	1.81,1.81, 1.84,1.85
	KGa	1.81,1.82, 1.84,1.85	1.81,1.81, 1.84,1.86	1.81,1.83, 1.85,1.86	1.80,1.83, 1.85,1.86	1.79,1.83, 1.84,1.87	1.81,1.81, 1.83,1.85	1.80,1.81, 1.84,1.86
Y–O (Å), Y= Li, Na, K, H	HB	0.99	0.98	0.99	0.99	0.98	0.98	0.99
	LiB	1.94	2.06	1.92	1.95	1.98	1.97	2.04
	NaB	2.25	2.44	2.36	2.42	2.31	2.25	2.36
	KB	2.62	2.69	2.76	2.75	2.65	2.65	2.92
	HAl	0.99	0.99	0.99	1.03	1.02	0.99	1.01
	LiAl	1.94	1.94	1.89	1.95	1.95	1.95	2.15
	NaAl	2.24	2.26	2.35	2.31	2.45	2.27	2.41
	KAl	2.64	2.63	2.81	2.74	2.70	2.68	2.77
	HGa	0.99	0.99	0.99	1.03	1.02	1.00	1.01
	LiGa	1.88	1.87	1.92	1.88	1.91	2.03	1.92
	NaGa	2.24	2.23	2.27	2.27	2.21	2.28	2.20
	KGa	2.62	2.61	2.68	2.70	2.60	2.63	2.68
cell volume ($Å^3$)	HB	3026.70	3027.19	3021.38	3018.24	3032.12	3071.33	3024.04
	LiB	2986.21	2986.75	2999.78	2946.81	2962.66	2988.85	2999.82
	NaB	3015.66	3017.42	2988.07	2975.79	3130.93	2994.57	3019.70
	KB	3006.72	3121.31	3018.68	3132.34	3137.90	2992.63	3117.40
	HAl	3066.28	3022.63	3059.37	3046.41	3047.32	3020.42	3018.32
	LiAl	3003.73	2992.06	3013.18	3009.80	2979.91	3025.10	3008.71
	NaAl	3046.95	3040.66	3026.92	3051.48	3046.91	3044.96	3047.19
	KAl	3051.04	3000.03	3027.09	3033.02	3040.47	3035.41	3022.22
	HGa	3026.26	3013.06	3051.74	3044.02	3049.46	3025.79	3046.07
	LiGa	3025.22	3009.37	3015.84	2977.24	2970.85	3023.93	2992.66
	NaGa	3013.87	3021.13	3024.99	3039.23	3042.46	3027.59	3006.97
	KGa	3011.44	3005.22	3030.62	3027.21	3044.39	3050.52	3014.70

a) The p(1×2×1) cell volume of the silica-MTW type zeolite is 3173.39 $Å^3$

Figure 1. The supercell of MTW-type zeolite. The Si and O atoms are shown in yellow (indexed with numbers 1–7) and red (indexed with letters a–k), respectively. The Si(1, 2, 3, 4, 5, 6 and 7) atoms are correspond to the T1, T3, T7, T6, T4, T2 and T5 sites of the International Zeolite Association web page, respectively.

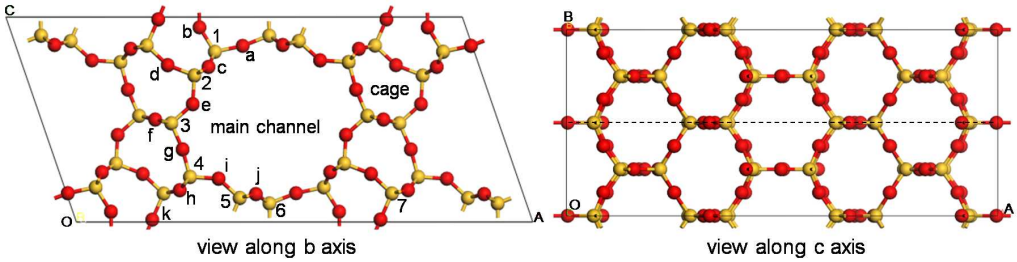

Figure 2. Local structures and relative energies (eV) for B-MTW zeolites. H, Li, Na, K, O, B, and Si atoms are in white, dark gray, violet, darkslateblue, red, green and yellow respectively. For the H-, Li-, Na-, and K-forms B-MTW zeolites, the relative energies of the most stable structure 0 eV, and the relative energies of the other structures are given with respective to the most stable structure. (Only related atoms were selectively shown for good viewing)

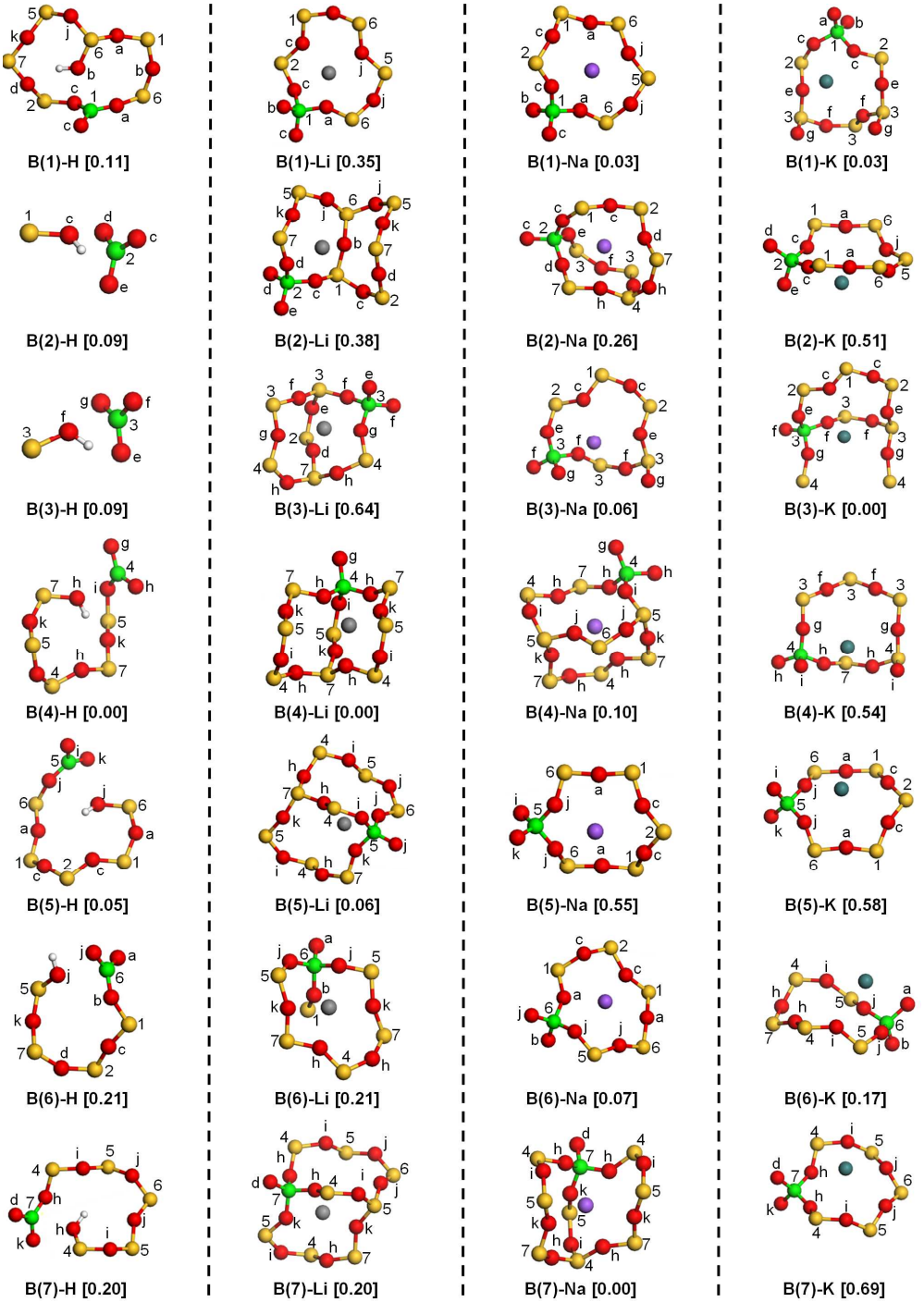

Figure 3. Local structures and relative energies (eV) for Al-MTW zeolites. H, Li, Na, K, O, Al, and Si atoms are in white, dark gray, violet, darkslateblue, red, gray and yellow respectively. For the H-, Li-, Na-, and K-forms Al-MTW zeolites, the relative energies of the most stable structure 0 eV, and the relative energies of the other structures are given with respective to the most stable structure. (Only related atoms were selectively shown for good viewing)

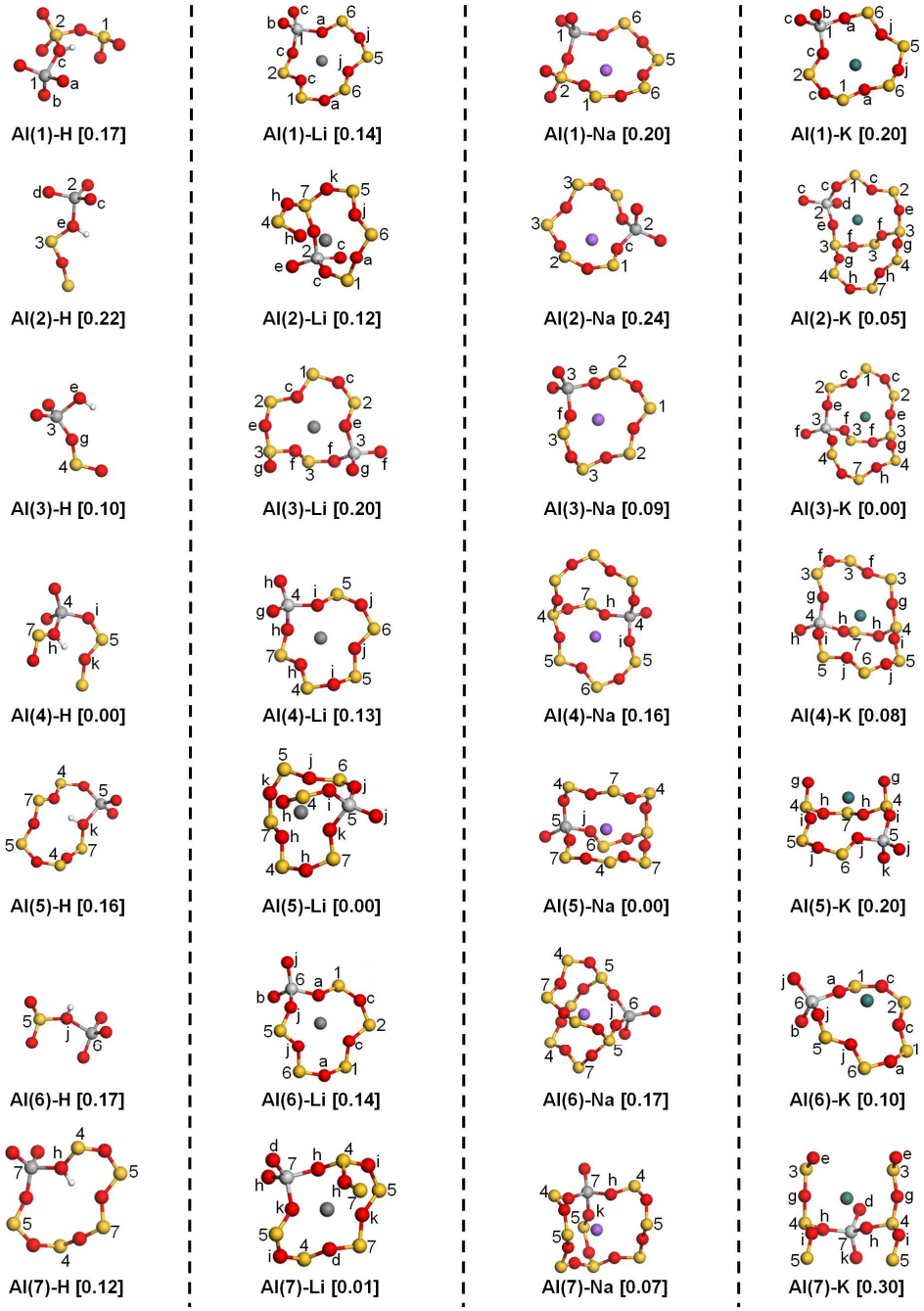

Figure 4. Local structures and relative energies (eV) for Ga-MTW zeolites. H, Li, Na, K, O, Ga, and Si atoms are in white, dark gray, violet, darkslateblue, red, tan and yellow respectively. For the H-, Li-, Na-, and K-forms Ga-MTW zeolites, the relative energies of the most stable structure 0 eV, and the relative energies of the other structures are given with respective to the most stable structure. (Only related atoms were selectively shown for good viewing)

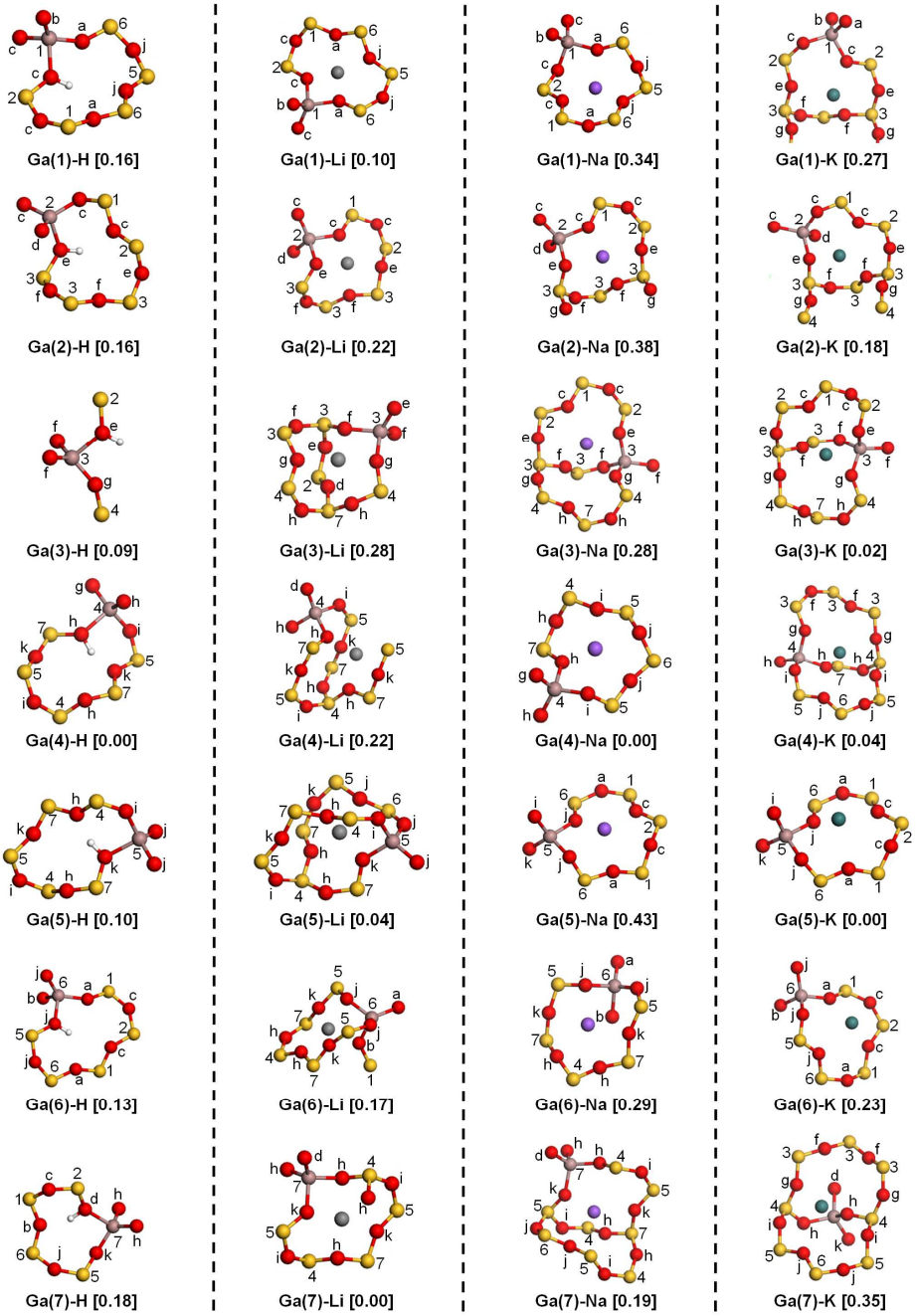

Figure 5. Energy as a function of the volume for the pure silica and B, Al and Ga incorporated *p*(1×2×1) MTW zeolites cell. Both the cell shape and ion positions are fully relaxed with fixed volumes.

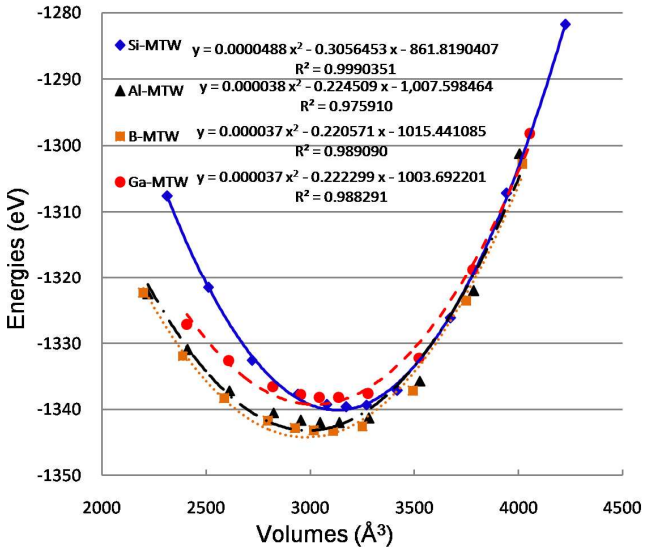

Figure 6. Contour plots of the electron density for Si, B, Al and Ga in the T sites of MTW zeolite. The plots (a), (b), (c), (d), (e), (f) and (g) are obtained from the plane containing the O(h)-Si(4)-O(i), B(7)-O(k)-Na, O(h)-B(4)-O(g), Al(4)-O(h)-H, Al(5)-O(j)-Na, Ga(4)-O(h)-H and Ga(4)-O(h)-Na, respectively.

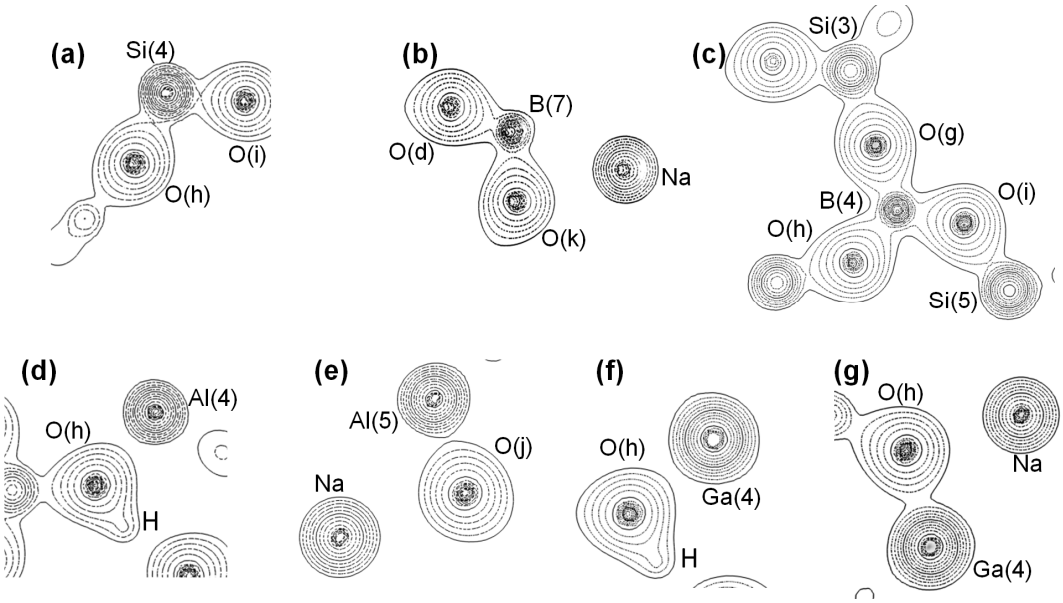

Figure 7. Local structures and adsorption energies (eV) for the adsorption of NH_3 and pyridine in B, Al and Ga incorporated H-form MTW zeolites. H, C, N, O, B, Al, Ga and Si atoms are shown in white, black, blue, red, green, gray, tan and yellow, respectively (Only related atoms were selectively shown for good viewing).

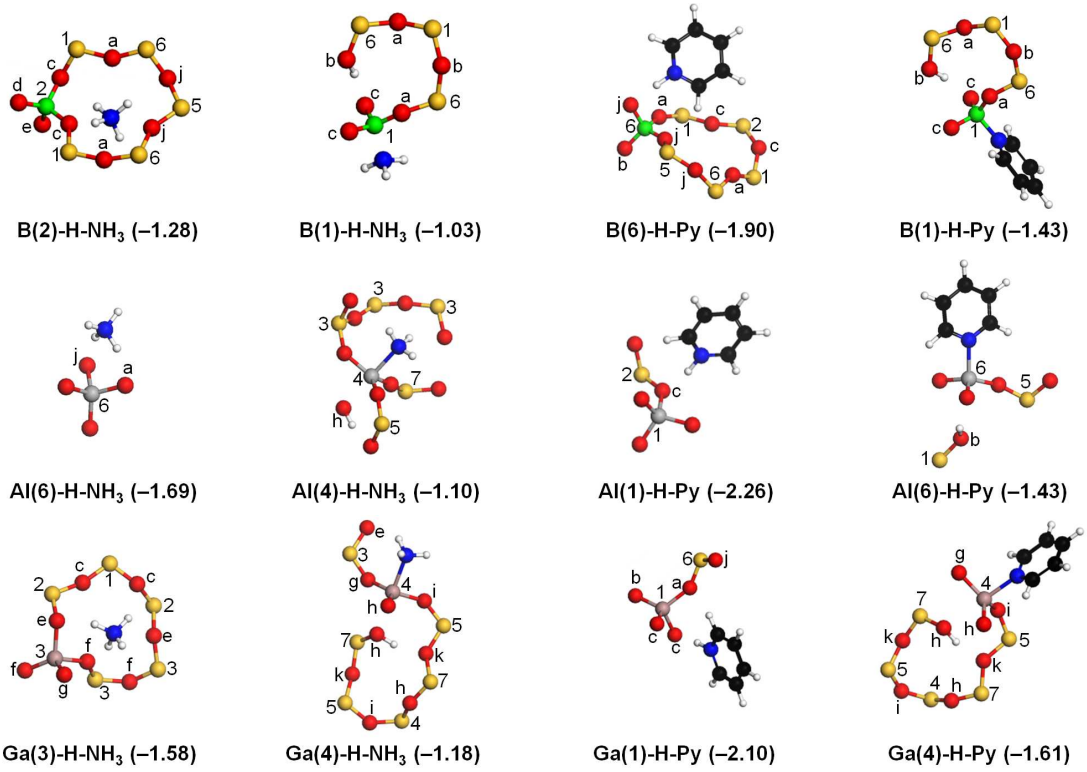

References

1 X. Meng, F.-S. Xiao, Green Routes for Synthesis of Zeolites, *Chem. Rev.* 2013, **114**, 1521-1543.

2 C. S. Cundy, P. A. Cox, The Hydrothermal Synthesis of Zeolites: History and Development from the Earliest Days to the Present Time, *Chem. Rev.* 2003, **103**, 663-702.

3 A. Corma, From Microporous to Mesoporous Molecular Sieve Materials and Their Use in Catalysis, *Chem. Rev.* 1997, **97**, 2373-2420.

4 E.J. Rosinski, M.K. Rubin, US Patent 3832,449, 1974.

5 R. B. LaPierre, A. C. Rohrman jr, J. L. Schlenker, J. D. Wood, M. K. Rubin, W. J. Rohrbaugh, The Framework Topology of ZSM-12: a High-silica Zeolite, *Zeolites* 1985, **5**, 346-348.

6 C. A. Fyfe, H. Gies, G. T. Kokotailo, B. Marler, D. E. Cox, Crystal Structure of Silica-ZSM-12 by the Combined use of High-resolution Solid-state MAS NMR Spectroscopy and Synchrotron X-ray Powder Diffraction, *J. Phys. Chem.* 1990, **94**, 3718-3721.

7 L. Dimitrov, M. Mihaylov, K. Hadjiivanov, V. Mavrodinova, Catalytic Properties and Acidity of ZSM-12 Zeolite with Different Textures, *Microporous Mesoporous Mater.* 2011, **143**, 291-301.

8 B. Gil, Ł. Mokrzycki, B. Sulikowski, Z. Olejniczak, S. Walas, Desilication of ZSM-5 and ZSM-12 Zeolites: Impact on Textural, Acidic and Catalytic Properties, *Catal. Today* 2010, **152**, 24-32.

9 A. O. S. Silva, M. J. B. Souza, J. Aquino, V. J. Fernandes, A. S. Araujo, Acid Properties of the HZSM-12 Zeolite with Different Si/Al Ratio by Thermo-programmed Desorption, *J. Therm. Anal. Calorim.* 2004, **76**, 783-791.

10 G. Košová, J. Čejka, Incorporation of Aluminum and Iron into the ZSM-12 Zeolite: Synthesis and Characterization of Acid Sites, *Collect. Czech. Chem. Commun.* 2002, **67**,

1760-1778.

11 W. Zhang, E. C. Burckle, P. G. Smirniotis, Characterization of the Acidity of Ultrastable Y, Mordenite, and ZSM-12 via NH_3-stepwise Temperature Programmed Desorption and Fourier Transform Infrared Spectroscopy, *Microporous Mesoporous Mater.* 1999, **33**, 173-185.

12 W. Zhang, P. G. Smirniotis, M. Gangoda, R. N. Bose, Brønsted and Lewis Acid Sites in Dealuminated ZSM-12 and β Zeolites Characterized by NH_3-STPD, FT-IR, and MAS NMR Spectroscopy, *J. Phys. Chem. B* 2000, **104**, 4122-4129.

13 Ł. Mokrzycki, B. Sulikowski, Z. Olejniczak, Properties of Desilicated ZSM-5, ZSM-12, MCM-22 and ZSM-12/MCM-41 Derivatives in Isomerization of α-pinene, *Catal. Lett.* 2009, **127**, 296-303.

14 R. Millini, F. Frigerio, G. Bellussi, G. Pazzuconi, C. Perego, P. Pollesel, U. Romano, A Priori Selection of Shape-selective Zeolite Catalysts for the Synthesis of 2,6-dimethylnaphthalene, *J. Catal.* 2003, **217**, 298-309.

15 J. G. de Almeida, M. Dufaux, Y. Ben Taarit, C. Naccache, Effect of Pore Size and Aluminium Content on the Production of Linear Alkylbenzenes over HY, H-ZSM-5 and H-ZSM-12 Zeolites: Alkylation of Benzene with 1-dodecene, *Appl. Catal., A* 1994, **114**, 141-159.

16 W. Wu, W. G. Wu, O. V. Kikhtyanin, L. F. Li, A. V. Toktarev, A. B. Ayupov, J. F. Khabibulin, G. V. Echevsky, J. Huang, Methylation of Naphthalene on MTW-type Zeolites. Influence of Template Origin and Substitution of Al by Ga, *Appl. Catal., A* 2010, **375**, 279-288.

17 X. F. Bai, K. Y. Sun, W. Wu, P. F. Yan, J. Yang, Methylation of Naphthalene to Prepare 2,6-dimethylnaphthalene over Acid-dealuminated HZSM-12 Zeolites, *J. Mol. Catal. A: Chem.* 2009, **314**, 81-87.

18 Q. Wang, Z.-M. Cui, C.-Y. Cao, W.-G. Song, 0.3 Å Makes the Difference: Dramatic

Changes in Methanol-to-olefin Activities Between H-ZSM-12 and H-ZSM-22 Zeolites, *J. Phys. Chem. C* 2011, **115**, 24987-24992.

19 X. Wei, P. G. Smirniotis, Synthesis and Characterization of Mesoporous ZSM-12 by Using Carbon Particles, *Microporous Mesoporous Mater.* 2006, **89**, 170-178.

20 A. Araujo, A. Silva, M. Souza, A. Coutinho, J. Aquino, J. Moura, A. Pedrosa, Crystallization of ZSM-12 Zeolite with Different Si/Al Ratio, *Adsorption* 2005, **11**, 159-165.

21 I. Kinski, P. Daniels, C. Deroche, B. Marler, H. Gies, Structure and Properties of the Composite Zeolite Silica-ZSM-12/para-nitroaniline, *Microporous Mesoporous Mater.* 2002, **56**, 11-25.

22 S. Gopal, K. Yoo, P. G. Smirniotis, Synthesis of Al-rich ZSM-12 Using TEAOH as Template, *Microporous Mesoporous Mater.* 2001, **49**, 149-156.

23 S. Ernst, P. A. Jacobs, J. A. Martens, J. Weitkamp, Synthesis of Zeolite ZSM-12 in the System $(MTEA)_2O$-Na_2O-SiO_2-Al_2O_3-H_2O, *Zeolites* 1987, **7**, 458-462.

24 T. De Baerdemaeker, U. Müller, B. Yilmaz, Alkali-free Synthesis of Al-MTW Using 4-cyclohexyl-1,1-dimethylpiperazinium Hydroxide as Structure Directing Agent, *Microporous Mesoporous Mater.* 2011, **143**, 477-481.

25 A. Mitra, C. W. Kirby, Z. Wang, L. Huang, H. Wang, Y. Huang, Y. Yan, Synthesis of Pure-silica MTW Powder and Supported Films, *Microporous Mesoporous Mater.* 2002, **54**, 175-186.

26 N. K. Mal, A. Bhaumik, R. Kumar, A. V. Ramaswamy, Sn-ZSM-12, a New, Large Pore MTW Type Tin-silicate Molecular Sieve: Synthesis, Characterization and Catalytic Properties in Oxidation Reactions, *Catal. Lett.* 1995, **33**, 387-394.

27 Y. Kamimura, K. Iyoki, S. P. Elangovan, K. Itabashi, A. Shimojima, T. Okubo, OSDA-free Synthesis of MTW-type Zeolite from Sodium Aluminosilicate Gels with Zeolite Beta Seeds, *Microporous Mesoporous Mater.* 2012, **163**, 282-290.

28 Y. Kamimura, K. Itabashi, T. Okubo, Seed-assisted, OSDA-free Synthesis of MTW-type Zeolite and "Green MTW" from Sodium Aluminosilicate Gel Systems, *Microporous Mesoporous Mater.* 2012, **147**, 149-156.

29 K. Iyoki, Y. Kamimura, K. Itabashi, A. Shimojima, T. Okubo, Synthesis of MTW-type Zeolites in the Absence of Organic Structure-directing Agent, *Chem. Lett.* 2010, **39**, 730-731.

30 M.-Y. Song, W.-Z. Zhou, Y.-C. Long, Preparation and Charactrization of Fibrous Crystals of Boron-containing MTW-type Zeolite, *Chin. J. Chem.* 2004, **22**, 119-121.

31 Y.-X. Zhi, A. Tuel, Y. B. Taarit, C. Naccache, Synthesis of Gallosilicates - MTW- type Structure Zeolites: Evidence of Ga-substituted T Atoms, *Zeolites* 1992, **12**, 138-141.

32 R. Millini, G. Perego, G. Bellussi, Synthesis and Characterization of Boron-containing Molecular Sieves, *Top. Catal.* 1999, **9**, 13-34.

33 A. Chatterjee, A. K. Chandra, Fe and B Substitution in ZSM-5 Zeolites: a Quantum-mechanical Study, *J. Mol. Catal. A: Chem.* 1997, **119**, 51-56.

34 S. Yuan, J. Wang, Y. Li, S. Peng, Siting of B, Al, Ga or Zn and Bridging Hydroxyl Groups in Mordenite: an Ab Initio Study, *J. Mol. Catal. A: Chem.* 2001, **175**, 131-138.

35 C. T. W. Chu, C. D. Chang, Isomorphous Substitution in Zeolite Frameworks. 1. Acidity of Surface Hydroxyls in [B]-, [Fe]-, [Ga]-, and [Al]-ZSM-5, *J. Phys. Chem.* 1985, **89**, 1569-1571.

36 A. Navrotsky, O. Trofymluk, A. A. Levchenko, Thermochemistry of Microporous and Mesoporous Materials, *Chem. Rev.* 2009, **109**, 3885-3902.

37 G. Feng, Z.-H. Lu, D. Kong, D. Yang, H. Guo, J. Liu, First Principle Calculation Evaluations for MTW-type Zeolites Synthesis Prescriptions, *Chem. Lett.* 2014, **43**, 1026–1028.

38 G. Feng, Y.-Y. Lian, D. Yang, J. Liu, D. Kong, Distribution of Al and Adsorption of NH_3 and Pyridine in ZSM-12: a Computational Study, *Can. J. Chem.* 2013, **91**, 925-934.

39 G. Feng, Z.-H. Lu, D. Kong, D. Yang, J. Liu, A First Principle Study on Fe Incorporated MTW-type Zeolite, *Microporous Mesoporous Mater.* 2014, **accepted**.

40 R. Aiello, F. Crea, E. Nigro, F. Testa, R. Mostowicz, A. Fonseca, J. B. Nagy, The Influence of Alkali Cations on the Synthesis of ZSM-5 in Fluoride Medium, *Microporous Mesoporous Mater.* 1999, **28**, 241-259.

41 G. Kresse, J. Furthmüller, Efficiency of Ab-initio Total Energy Calculations for Metals and Semiconductors Using a Plane-wave Basis Set, *Comput. Mater. Sci.* 1996, **6**, 15-50.

42 G. Kresse, J. Furthmüller, Efficient Iterative Schemes for Ab Initio Total-energy Calculations Using a Plane-wave Basis Set, *Phys. Rev. B* 1996, **54**, 11169-11186.

43 S. Grimme, Semiempirical GGA-type Density Functional Constructed with a Long-range Dispersion Correction, *J. Comput. Chem.* 2006, **27**, 1787-1799.

44 J. P. Perdew, K. Burke, M. Ernzerhof, Generalized Gradient Approximation Made Simple, *Phys. Rev. Lett.* 1996, **77**, 3865-3868.

45 P. E. Blöchl, C. J. Forst, J. Schimpl, Projector Augmented Wave Method: Ab Initio Molecular Dynamics with Full Wave Functions, *Bull. Mater. Sci.* 2003, **26**, 33-41.

46 P. E. Blöchl, Projector Augmented-wave Method, *Phys. Rev. B* 1994, **50**, 17953-17979.

47 T. s. Bučko, J. r. Hafner, S. b. Lebègue, J. n. G. Ángyán, Improved Description of the Structure of Molecular and Layered Crystals: Ab Initio DFT Calculations with van der Waals Corrections, *J. Phys. Chem. A* 2010, **114**, 11814-11824.

48 S. Svelle, C. Tuma, X. Rozanska, T. Kerber, J. Sauer, Quantum Chemical Modeling of Zeolite-Catalyzed Methylation Reactions: Toward Chemical Accuracy for Barriers, *J. Am. Chem. Soc.* 2009, **131**, 816-825.

49 K. Yoo, R. Kashfi, S. Gopal, P. G. Smirniotis, M. Gangoda, R. N. Bose, TEABr Directed Synthesis of ZSM-12 and Its NMR Characterization, *Microporous Mesoporous Mater.* 2003, **60**, 57-68.

50 J. E. Huheey, E. A. Keiter, R. L. Keiter, O. K. Medhi, *Inorganic Chemistry: Principles of Structure and Reactivity*, Pearson Education, 2006.

51 R. P. Stoffel, C. Wessel, M.-W. Lumey, R. Dronskowski, Ab Initio Thermochemistry of Solid-State Materials, *Angew. Chem., Int. Ed.* 2010, **49**, 5242-5266.

52 T. Demuth, J. Hafner, L. Benco, H. Toulhoat, Structural and Acidic Properties of Mordenite. An Ab Initio Density-functional Study, *J. Phys. Chem. B* 2000, **104**, 4593-4607.

53 H. Fujita, T. Kanougi, T. Atoguchi, Distribution of Brønsted Acid Sites on Beta Zeolite H-BEA: A Periodic Density Functional Theory Calculation, *Appl. Catal., A* 2006, **313**, 160-166.

54 K. Momma, F. Izumi, VESTA 3 for Three-dimensional Visualization of Crystal, Volumetric and Morphology Data, *J. Appl. Crystallogr.* 2011, **44**, 1272-1276.

55 S.-H. Wen, W.-Q. Deng, K.-L. Han, Endohedral BN Metallofullerene $M@B_{36}N_{36}$ Complex as Promising Hydrogen Storage Materials, *J. Phys. Chem. C* 2008, **112**, 12195-12200.

56 T. Xue, Y. M. Wang, M. Y. He, Facile Synthesis of Nano-sized NH_4-ZSM-5 Zeolites, *Microporous Mesoporous Mater.* 2012, **156**, 29-35.

57 N. Jiang, S. Yuan, J. Wang, Z. Qin, H. Jiao, Y.-W. Li, An ONIOM Study of Amines Adsorption in H-[Ga]MOR, *J. Mol. Catal. A: Chem.* 2005, **232**, 59-67.

58 N. Jiang, S. Yuan, J. Wang, H. Jiao, Z. Qin, Y.-W. Li, A Theoretical Study of Amines Adsorption in HMOR by Using ONIOM2 Method, *J. Mol. Catal. A: Chem.* 2004, **220**, 221-228.

59 P. Strodel, K. M. Neyman, H. Knözinger, N. Rösch, Acidic Properties of [Al], [Ga] and [Fe] Isomorphously Substituted Zeolites. Density Functional Model Cluster Study of the Complexes with a Probe CO Molecule, *Chem. Phys. Lett.* 1995, **240**, 547-552.

Graphical Abstract

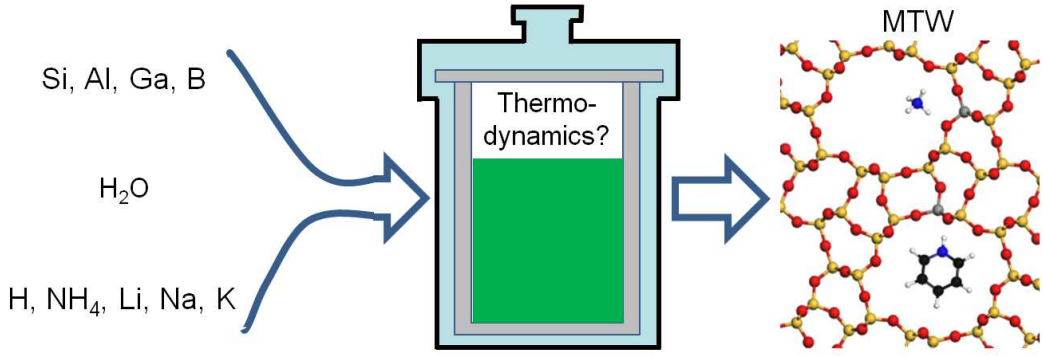

The synthesis prescriptions, structures and acid properties of B, Al and Ga incorporated MTW-type zeolites were studied at DFT level.